Evaluation of Effective Paramters on Formability of TWB

A. Nayebi[*] and A.H. Khosravi

Department of Mechanical Engineering, Shiraz University, Shiraz, Iran

Abstract: Formability of automotive friction stir welded TWB (tailor welded blank) sheets is numerically investigated in biaxial stretching based on hemispherical dome stretch (HDS) test in four automotive sheets of Aluminum alloy 6111-T4, 5083-H18, 5083-O and DP590 steel, having different thicknesses. The effects of the weld zone modeling and the thickness ratio on formability are evaluated. In order to carry out the numerical simulations, mechanical properties are considered according to Chung et al. [11] experimental results. von-Mises and Hill'48 quadratic yield functions are used to compare the isotropic and anisotropic behaviors of the used sheets. In order to simplify the problem, the anisotropy of the weld zone is ignored. The FEM results are compared with experimental results of [11]. Anisotropic assumption for base materials and varying thickness for the weld zone give more accurate prediction. Numerical results are in good agreement with the experimental results. Failure onset locations and patterns are accurate. Since the formability is dependent on the stress concentration, asymmetric distribution of strength and complexity of weld zone properties, the thickness ratio in TWB affect formability.

1. Introduction

In recent years, demand for light weight and/or high-strength sheet metals such as Aluminum alloys and advanced high strength steels, has steadily been increased in automotive applications. In order to save materials and reduce vehicle weight, automotive companies are developing Tailor-Welded Blank (TWB) made sheets. So far, TWBs can be made of blank sheets with different thickness, material properties and even surface coating with different friction coefficients. However, it still has several difficulties to fabricate TWB sheets, especially for aluminum alloy sheets because of their lower formability and less familiar weld ability requirements [1]. On the evaluation of formability of TWBs, Hemispherical Dome Stretch (HDS) test is one of the most popular ones. The HDS test includes punch, die and blank holder. Many researchers have modeled weld line simply and neglected weld geometry and/or their properties. Yuliang Shi et al. [2] assumed weld line with three simple representations. First, coincident nodal model neglecting the weld line. Second, the rigid link model, and third, two-fold beam element. Raymond et al. [3] represented that mesh element type was affected by changing the model of the parent metals from shell element to solid element. They included weld material properties with solid element and constrained them with parent material shell elements. Zhao et al. [4] assumed that 3-D shell element for parent metals and mid-plane of two sheets were considered along each other by modeling both weld line and HAZ (Heat Affected Zone). They neglected accurate geometry and/or material properties of weld and HAZ. Zadpoor [1, 5] tried to model weld and HAZ carefully by measuring and analyzing microstructure of the weld line. Furthermore, he followed the assumptions of Liu et al. [6], in which HAZ is included in the weld nugget. Raymond et al. [3], Zhao et al. [4], Shi et al. [2] and Chan et al. [7] analyzed TWB through isotropic models. However, due to rolling process of base materials, the material properties are different in rolling and transverse directions. Panda et al. [8] used three parameters

yield function by Barlet in order to describe anisotropic behavior of IF steel TWB. Zadpoor [1, 5] used Hill's 48 yield criterion and Hollomon's hardening law for 2024-T3 and 7075-T6 aluminum alloys. Manabhan et al. [9] used Hooke's law in the elastic region. Strain hardening was described by Swift's law ($\overline{\sigma} = K(\varepsilon_0 + \overline{\varepsilon}^p)^n$) and Hill's 48 quadratic yield criterion to describe the plastic behavior of steel blank sheets and the weld line. The yield criterion of Cazacu and Barlat was used for materials with low r-values to describe the plastic behavior of aluminum alloy sheets. Daeyong Kim et al. [10] implemented the non-quadratic orthogonal anisotropic yield function, Yld 2004-18P, and the Voce and/or Hollomon's hardening was used to model the isotropic hardening. Studies have shown that because of complexity of crystal patterns in weld zone and HAZ, it is not possible to describe these zones perfectly (especially for FSW) [1]. Hence, anisotropy and inhomogeneity are inevitable. Manabhan et al [9] simulated weld zone by a rule of mixture. Thus, there are three approaches to consider weld zone; neglect weld zone, weld zone geometry alone, and both weld zone geometry and material property simultaneously.

In this study, the macroscopic formability performance of automotive friction stir welded TWB sheets is numerically investigated. Four automotive sheets, aluminum alloy 6111-T4, 5083-H18, 5083-O and DP590 steel sheets, with one or two different thicknesses are studied. Simulation results are compared with the experimental results. Based on FLDs, failure onset and pattern on test specimens are also evaluated and compared with the experimental results.

2. Material Properties

Four automotive sheets were welded along the rolling direction by friction-stir welding method [11]. In this research, the same materials with the same thickness (similar gauges, SG) and different thickness (dissimilar gauges, DG) were welded together (Table 1). Material properties and the stress − strain hardening curves were obtained from simple tension tests (Table 2). K and n are hardening coefficient and hardening exponent, respectively. Voce's model constants are A, B and C according to $\overline{\sigma} = A + B(1 - \exp(-C\overline{\varepsilon}))$. Since stretching is dominant and unloading behavior is insignificant in this test, the isotropic hardening law is used without considering kinematic hardening behavior. von-Mises (Eq. 1) and Hill's48 quadratic yield functions (Eq. (2)) are considered and the anisotropy of the weld zone was ignored for simplicity.

$$f(\sigma) = \sqrt{1/2\left[(\sigma_{11} - \sigma_{22})^2 + (\sigma_{11} - \sigma_{33})^2 + (\sigma_{22} - \sigma_{33})^2 + 6\sigma_{12}^2 + 6\sigma_{13}^2 + 6\sigma_{23}^2\right]} \tag{1}$$

$$f(\sigma) = \sqrt{F(\sigma_{22} - \sigma_{33})^2 + G(\sigma_{33} - \sigma_{11})^2 + H(\sigma_{11} - \sigma_{22})^2 + 2L(\sigma_{23})^2 + 2M(\sigma_{13})^2 + 2N(\sigma_{12})^2} \tag{2}$$

where σ_{ij} (i=j) are normal stresses and σ_{ij} (i≠j) are shear stresses in global coordinate system and F, G, H, L, M and N are material constants which were determined by the in-plane testing results [11] (Table 3). Hemispherical dome stretching test is a plane stress processing. Thus, L and M coefficients in Eq. (2) don't have any effect on the mentioned problem.

Forming limit diagrams (FLDs) were measured for base materials and calculated for the weld zones [11] (Fig. 1). The Voce type FLD is considered for 6111-T4, 5083-H18 and the Hollomon type FLD is used for 5083-O, DP590 weld zones. Based on the material properties including the forming limit diagrams, the formability of FSW sheets are numerically investigated for hemispherical dime stretching test.

3. FE Simulation of the Hemispherical Dome Stretching Tests

In order to investigate the formability of FSW sheets in biaxial stretching deformation, hemispherical dome stretching (HDS or FLD) tests were performed with four welded samples by Chung et al. [11]: 6111-T4 (SG, DG), 5083-H18 (SG, DG),AA5083-O (SG) and DP-steel (SG) (details of the experimental results were given

in [11]). With the help of the material properties, the constitutive law for the isotropic hardening behavior and the Hill's48 quadratic yield function are used in the FEM code (ABAQUS).

Table 1. Thicknesses of base materials and the combination of thicknesses for welded specimens.

Materials	Base materials		Welded specimens	
	Thin(mm)	Thick(mm)	SG(mm)	DG(mm)
6111-T4	1.5	2.6	1.5-1.5	1.5-2.6
5083-H18	1.2	1.6	1.6-1.6	1.2-1.6
5083-O	1.6		1.6-1.6	
DP590	1.5	2.0	2.0-2.0	1.5-2.0

Table 2. Isotropic hardening description.

Materials			Voce		
			A(MPa)	B(MPa)	C
6111-T4	Base	1.5t	165.9	212.8	9.373
		2.6t	172.8	206.3	9.900
	Weld	SG	167.59	144.30	12.58
		DG	151.25	103.03	21.21
5083-H18	Base	1.2t	397.6	120.0	14.120
		1.6t	388.6	123.0	15.133
	Weld	SG&DG	172.57	251.43	10.8
5083-O	Base	1.6t	144.0	227.8	12.093
	Weld	SG	178.76	227.49	13.29

Materials			Hollomon	
			K(MPa)	n
DP590	Base	1.5t	1072.1	0.171
		2.0t	1043.6	0.173
	Weld	SG	1136.71	0.104
		DG	1064.33	0.115

Table 3. Anisotropic coefficients of Hill'48 quadratic function.

Materials Gauge(mm)	6111-T4		5083-H18		5083-O	DP590
	1.5t	2.6t	1.6t	1.2t	1.6t	2.0t
F	0.54248	0.54699	0.45533	0.45624	0.51635	0.49069
G	0.45759	0.50999	0.49574	0.49833	0.48444	0.50671
H	0.54248	0.49008	0.50442	0.50179	0.51639	0.49325
N	1.53085	1.60224	1.84090	1.72900	1.61887	1.63704

Even though hemispherical dome stretching test can introduce various biaxial strain modes, only one type of the strain mode is considered here, except for 5083-H18. Initial dimensions of the rectangular blank sheets are 200mm×200mm. This is near balanced biaxial mode, while longitudinal weld lines were aligned parallel to the rolling direction. Because of the brittle nature of 5083-H18 (SG) and (DG), the initial clamping leads to the fracture at the draw bead position. Hence, 200mm×120mm blank test was successfully performed using a flat grooved bead instead of the general circular shaped draw one. LDH at the fracture were measured and failure onset locations were also observed. Analytical rigid surface in simulation is utilized for the tools as the punch, the holder and the die (geometry details of assembly are given in [12]). Simulations of 6111-T4, 5083-O and DP590 TWB sheets are performed with the exact draw bead shape while, the simulation of 5083-H18 test is carried out without a draw bead.

The reduced four node shell element S4R with five integration points through thickness is employed to model the blank. The element sizes are selected in a manner that satisfies convergences, computational cost and accurate results. 6111-T4 (SG, DG), 5083-O (SG), DP-steel (SG) are meshed by 2796 elements and 2888 nodes and 5083-H18 (SG, DG) are meshed by 2786 elements and 2872 nodes which shows a reasonable mesh refinement. Only half blank are simulated with consideration of the symmetric boundary condition. In this study, anisotropic yield surface is considered and weld zone properties as well as weld zone geometry are included in the numerical analysis and are compared with the isotropic von-Mises yield function. Forming limit diagrams, which have been ignored in the majority of the previous works are considered for both the base and the weld. In order to compare the performance of the modeling, three simulation methods are used (Fig. 2). Model- A is perfect welding condition (therefore, the weld zone is ignored completely), model-B is average mechanical property of the weld zone with uniform average weld zone thickness [4] and model-C is average weld zone property with varying weld zone thickness. The friction coefficient for the lubricated condition is considered 0.08 between the punch and the blank in all cases. Between the die/holder and the blank, the coefficient of friction is 0.16 for the non-lubricated. In order to describe the flat grooved bead without draw bead except 5083-H18, the coefficient of friction is considered as 0.2. It is assumed that the base sheets and the weld geometry are in the same plane at the sheet face and it doesn't touch the punch.
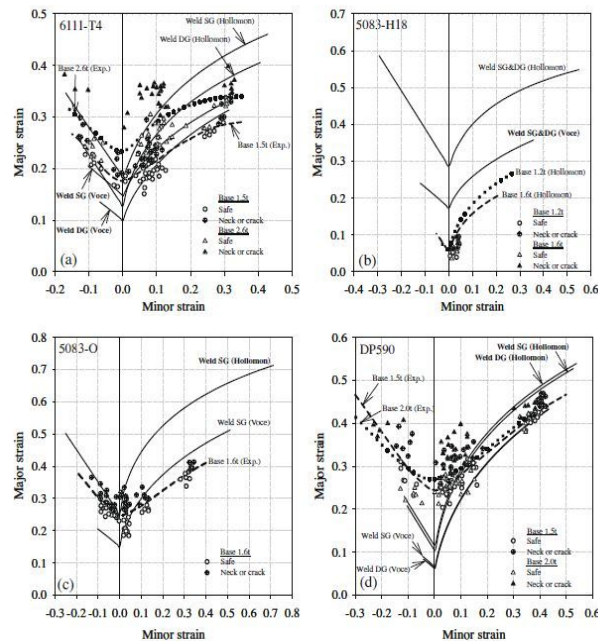

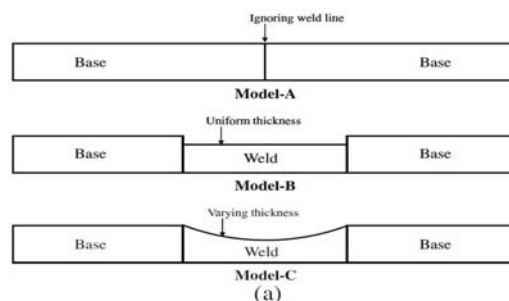Fig. 1. Forming limit diagrams: (a) 6111-T4; (b) 5083-H18; (c) 5083-O; and (d) DP590 [11].

Fig. 2. Schematic view of the three types of weld models

4. Results and Discussions

4.1. Weld line modeling with the assumption of isotropic and anisotropic behavior of base materials

The LDH values of TWBs are determined (Table 4) by FLD approach. Isotropic and anisotropic behavior of base materials in the modeling of the weld line of SG are considered in the three different models of A, B and C. DG samples are modeled with C-type and compared with experimental values [10]. In order to enhance more accurate results, model C with the anisotropic behavior is used.

4.2. Failure onset locations and patterns

Plastic anisotropic behavior of sheets is considered in order to predict the failure onset location better and the modeling prediction is compared with the experimental results in Figs. 3 to 8. The experimental failure of the 6111-T4 (SG) occurred in the weld zone parallel to the weld line, even though the retreating side of the weld zone is thinner in the middle zone. Failure in simulation occurred in the base material beside the weld zone and perpendicular to the weld line (Fig. 3). This discrepancy is due to the inaccuracy on the weld line geometry and HAZ properties which is brittle. Both experimental and simulation failure of 6111-T4 (DG) occurred at retreating side of the weld zone (Fig. 4). The 5083-H18 (SG) failed in a point near and along the rim, where the punch contacts the sheet in the last step. The failure is perpendicular to the weld line in the experimental results as well as in the simulation result (Fig. 5). According to the simulation, failure initiated at the base material in 5083-H18 (SG) specimen, since the weld zone of 5083-H18 material is more ductile than its base material. Failure of 5083-H18 (DG) was initiated in the thinner base material and perpendicular to the weld line in both experimental and simulated results (Fig. 6). The failure in the experiment and in the simulation of 5083-O occurred near the rim area where the punch contacts the blank in the last region (Fig. 7). The simulation results show that failure starts at the base metal. This result is achieved because of more ductility of the weld zone with respect to the base material. The experimental and simulated failure line of DP 590 is observed parallel to the weld line that is near the boundary between the base region and the weld zone. However, the failure is out of the weld line in the experimental test and it is inside of the weld line in the simulation of the test (Fig. 8). This discrepancy might be associated with the accuracy of the weld zone simulation and the assumption of the average properties of HAZ.

Table 4. Dome height (mm) in hemispherical dome stretching tests
obtained by the simulation and experimental tests.

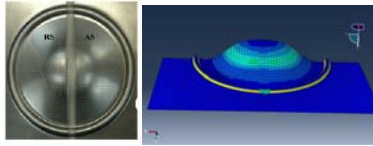| Materials		Model	LDH(sim, iso)(mm)	LDH(sim, aniso)(mm)	LDH(exp)(mm)
6111-T4	SG	A	17.54	-	-
		B	18.047	-	-
		C	18.21	17.47	17.9($\pm$1.6)
	DG	C	9.912	10.67	12.7($\pm$2.3)
5083-H18	SG	A	12.289	-	-
		B	14.339	-	-
		C	14.85	15.205	17.0($\pm$1.6)
	DG	C	13.37	14.54	16.9($\pm$1.4)
5083-O	SG	A	24.62	-	-
		B	25.31	-	-
		C	25.48	26.01	27.6($\pm$0.8)
DP590	SG	A	15.556	-	-
		B	7.59	-	-
		C	9.58	10.47	11.9($\pm$1.0)

Fig. 3. Experimental [11] and simulated (model-C, anisotropic) failure onset for 6111-T4(SG)
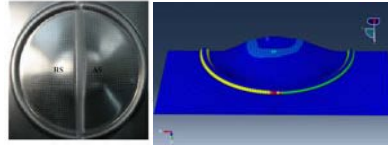

Fig. 4. Experimental [11] and simulated (model-C, anisotropic) failure onset for 6111-T4(DG)
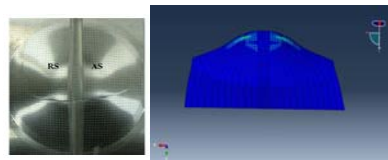

Fig. 5. Experimental [11] and simulated (model-C, anisotropic) failure onset for 5083-H18(SG)
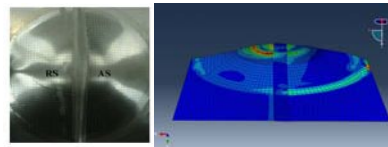

Fig. 6. Experimental [11] and simulated (model-C, anisotropic) failure onset for 5083-H18(DG).
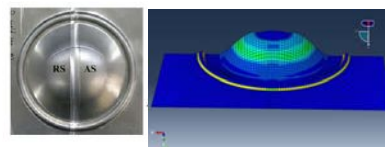

Fig. 7. Experimental [11] and simulated (model-C, anisotropic) failure onset for 5083-O(SG).
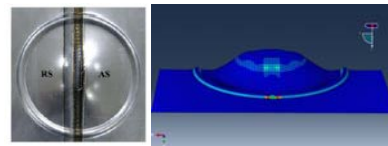

Fig. 8. Experimental [11] and simulated (model-C, anisotropic) failure onset for DP590 (SG).

5. Conclusion

Formability performance of the automotive friction stir welded TWB sheets in the hemispherical dome stretching test is numerically investigated for three aluminum alloys (6111-T4, 5083-H18, 5083-O) and DP590 welded sheets. Anisotropy/isotropy behavior in the yield stress and the weld zone properties as well as the geometry and forming limit diagrams are considered in numerical simulations. Since strain localization is highly dependent on thickness variation in the specimen and mechanical behavior, detailed description of the weld zone thickness geometry in the numerical study is as important as the base materials yield behavior (isotropy or anisotropy). Anisotropic assumption for the base materials and varying thickness for the weld zone give more accurate prediction of the forming failure. Numerical results agreed reasonably well with the experimental results. Prediction of the failure onset locations and their patterns are acceptable except the results of 6111-T4 (SG) specimen. This discrepancy is mainly occurred by the inaccurate weld zone property. The assumed uniform geometry and isotropic properties

assumption of the weld zone lead to the inaccuracy. Thickness ratio in TWB affects the formability because of stress concentration, asymmetric distribution of the strength and the complexity of weld zone properties.

5. References

[1] A. Zadpoor, Tailor-made blanks for the aircraft industry, Ph.D thesis, Delf university, (2010).

[2] Y. Shi, Z. Lin, P. Zhu and S. Han, Impact modeling of the weld line of tailor-welded blank, *Materials and Design*, 29 (2008) 232–238.

[3] S. D. Raymond, P. M. Wild and C. J. Bayley, On modeling of the weld line in finite element analyses of tailor welded blank forming operations, *Journal of Materials Processing Technology*, 147 (2004), 28–37.

[4] K. M. Zhao, B. K. Chun and J. K. Lee, Finite element analysis of tailor-welded blanks. *Finite Elements in Analysis and Design*, 37(2) (2001) 117–130.

[5] A. Zadpoor, J. Sinke and R. Benedictus, Finite element modeling and failure prediction of friction stir welded blanks, *Materials and Design*, 30 (2009) 1423–1434.

[6] G. Liu, L. E. Murr, C. S. Niou, J. C. McClure and F. R. Vega, Microstructural aspects of the friction-stir welding of 6061-T6 aluminum, *Scripta Mater*, 37 (1997) 355–361.

[7] S. M. Chan, L. C. Chan and T. C. Lee, Tailor-welded blanks of different thickness ratios effects on forming limit diagrams, *Journal of Materials Processing Technology*, Vol. 132(1–3) (2003) 95–101.

[8] S.K. Panda, D.R. Kumar, H. Kumar and A.K. Nath, Characterization of tensile properties of tailor welded IF steel sheets and their formability in stretch forming, *Journal of Materials Processing Technology*, 183 (2007) 321–332.

[9] R.P. Manabhan, M.C. Oliveira and L.F. Menezes, Deep drawing of aluminium–steel tailor-welded blanks, *Materials and Design*, Vol. 29 (2008) 154–160.

[10] D. Kim, W. Lee, J. Kim, K.H. Chung, C. Kim, K. Okamoto, R.H. Wagoner and K. Chung, Macro-performance evaluation of friction stir welded automotive tailor-welded blank sheets: Part II – Formability, *International Journal of Solids and Structures*, 47 (2010) 1063-1081.

[11] K. Chung, W. Lee, D. Kim, J. Kim, K. H.Chung, C. Kim, K. Okamoto and R. H. Wagoner, Macro-performance evaluation of friction stir welded automotive tailor-welded blank sheets: Part I – Material properties, *International Journal of Solids and Structures*, 47 (2010) 1048–1062.